JPE 19-5-23

https://doi.org/10.6113/JPE.2019.19.5.1303
ISSN(Print): 1598-2092 / ISSN(Online): 2093-4718

Study of Harmonic Suppression of Ship Electric Propulsion Systems

Yifei Wang[†,**], Youxin Yuan[*], and Jing Chen[*]

[†,*]School of Automation, Wuhan University of Technology, Wuhan, China
[**]University of Wisconsin-Madison, Madison, WI, USA

Abstract

This paper studies the harmonic characteristics of ship electric propulsion systems and their treatment methods. It also adopts effective measures to suppress and prevent ship power systems from affecting ship operation due to the serious damage caused by harmonics. Firstly, the harmonic characteristics of a ship electric propulsion system are reviewed and discussed. Secondly, aiming at problems such as resonant frequency and filter characteristics variations, resonance point migration, and unstable filtering performances in conventional passive filters, a method for fully tuning of a passive dynamic tunable filter (PDTF) is proposed to realize harmonic suppression. Thirdly, to address the problems of the uncontrollable inductance L of traditional air gap iron core reactors and the harmonics of power electronic impedance converters (PEICs), this paper proposes an electromagnetic coupling reactor with impedance transformation and harmonic suppression characteristics (ECRITHS), with the internal filter (IF) designed to suppress the harmonics generated by PEICs. The ECRITHS is characterized by both harmonic suppression and impedance change. Fourthly, the ECRITHS is investigated. This investigation includes the harmonic suppression characteristics and impedance transformation characteristics of the ECRITHS at the fundamental frequency, which shows the good performance of the ECRITHS. Simulation and experimental evaluations of the PDTF are carried out. Multiple PDTFs can be configured to realize multi-order simultaneous dynamic filtering, and can effectively eliminate the current harmonics of ship electric propulsion systems. This is done to reduce the total harmonic distortion (THD) of the supply currents to well below the 5% limit imposed by the IEEE-519 standard. The PDTF also can eliminate harmonic currents in different geographic places by using a low voltage distribution system. Finally, a detailed discussion is presented, with challenges and future implications discussed. The research results are intended to effectively eliminate the harmonics of ship electric power propulsion systems and to improve the power quality of ship power systems. This is of theoretical and practical significance for improving the power quality and power savings of ship power systems.

Key words: Dynamic tuning, Harmonic suppression, Power filter

I. INTRODUCTION

With the development of power electronics technology, variable frequency speed control technology, pod technology and digital technology based on microprocessors, ship electric propulsion systems have become strong competitors of diesel engines that directly drive the propeller propulsion system with their inherent advantages (such as maneuverability, reliability, and propulsion efficiency). Large-capacity power electronic devices are often employed in ship electric propulsion systems (such as rectification and inverter equipment). All power electronic devices generate a large amount of harmonics during power conversion and control, during which the propulsion is promoted and a large amount of power harmonics are injected into the grid [1], [2]. When a ship electric propulsion system is operating under different conditions, the harmonic content and waveform changes of the ship power system are different [3], [4]. Propulsion inverters serves as the main harmonic source of ship electric propulsion systems [5]. Harmonic content is increasing year by year [6], [7].

The fundamental power created by a generator is converted into the fundamental power flowing to the linear load and fundamental power flowing to the nonlinear load. At the

Manuscript received Mar. 6, 2019; accepted Apr. 19, 2019
Recommended for publication by Associate Editor Xiaoqiang Guo.
[†]Corresponding Author: wyfnhsz88@163.com
Tel: +86-13871397505, Wuhan University of Technology
[*]School of Automation, Wuhan University of Technology, China
[**]University of Wisconsin-Madison, USA

same time, the nonlinear load flows through part of its own fundamental power for absorption, with the other part being converted into harmonic power, which then flows to the system and linear load, and is then converted into heat energy, resulting in an increase in both the equipment capacity and circuit loss, a shortened life of electrical equipment, increasing energy loss of the power grid, and the possibility of resonance of the power system [8]. Harmonics can cause serious interference in communication and electronic equipment, which can result in a potential safety hazard, and problems in terms of the high quality and economic operation of a ship power system. Severe accidents caused by harmonics have occurred at home and abroad [9], [10]. Therefore, the harmonic problems in ship electric propulsion systems must be taken seriously. It is necessary to study these harmonics and their treatment methods, and to adopt effective measures to suppress and prevent ship power systems from affecting ship operation due to the serious damage caused by harmonics. The issue on how to effectively control harmonics below the 5% limit imposed by the IEEE-519 standard [11] while meeting the requirements of safe operation is an important and practical topic in the frontiers of scientific and technological workers.

A large number of experts and scholars at home and abroad have conducted in-depth research on harmonic suppression. The best way to solve the harmonic problem is to install a power filter at the nearest point to the harmonic source. There are three main methods depending on the class of filters: passive power filters (PPFs), active power filters (APFs), and hybrid power filters (HAPFs), which have their own strengths and weaknesses that make them suitable for different occasions, as shown in Table I. In short, these three power filters have their own advantages and disadvantages, which make them suitable for different occasions [12]-[25]. A lot of attention has been paid to developing a novel power filter, whose performance is basically the same as that of an active filter, while having a price advantage over the PDTF [10].

Existing studies on the harmonic suppressing technology of ship power systems focus mainly on harmonic characteristics, suppression research and the influence of converters on the current harmonics of ship power grids, which does not involve multi-order current harmonic suppression. Therefore, based on the study of the harmonic characteristics of a ship power system, an analysis is conducted in this paper from the perspective of PPF. This study focuses on the fact that the L/C parameters of PPF cannot be adjusted, and the poor filtering effect. Therefore, this paper puts forward an ECRITHS, which can optimize PDTFs, with the following organization. The harmonic characteristics of a ship electric propulsion system are reviewed and discussed in Section II. Section III proposes a method for fully tuning a PDTF. The harmonic suppression principle of the PDTF is analyzed in Section IV. The impedance transformation and harmonic suppression characteristics of the ECRITHS are studied in Section V. Simulation and experimental evaluations of a PDTF used for the harmonic suppression of a ship electric propulsion system are presented in Section VI. Section VII gives a detailed discussion and future research directions.

TABLE I
STRENGTHS AND WEAKNESSES OF DIFFERENT POWER FILTERS

Power filter	References	Strengths	Weaknesses
PPF	[12]-[15]	Simple structure Large capacity Low cost Stable performance	Large storage element Parallel resonances Not real time Greatly affected by the capacitor components
APF	[16]-[19]	High responsiveness High controllability Large capacity	Complex control system Expensive price High operating conditions
HAPFs	[20]-[24]	High efficiency Large capacity High controllability High reliability	Complex control algorithm High operating conditions Expensive price Height limitation of device

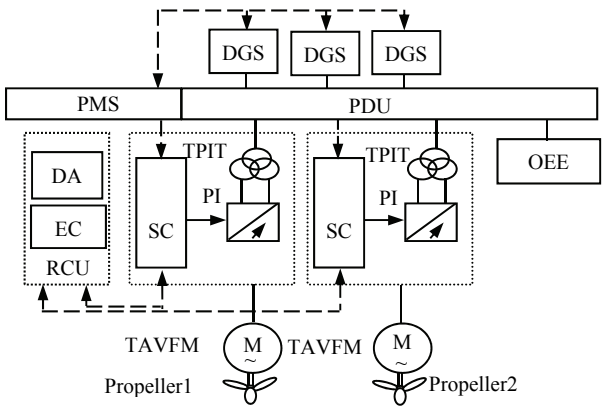

DGS: Diesel generator sets
PMS: Power station management system
PDU: Power distribution unit (main switchboard)
RCU: Remote control unit
DA: Detection alarm
EC: Emergency control
SC: System controller
PI: Propulsion inverter
TPIT: Three-phase isolation transformer
TAVFM: Three-phase AC variable frequency motor
OEE: Other electrical equipment

Fig. 1. Composition block diagram of a typical ship electric propulsion system.

II. HARMONIC CHARACTERISTICS OF A SHIP ELECTRIC PROPULSION SYSTEM

A ship power system, working as a whole, consists of power supply devices, power distribution devices, power grids and loads connected in a certain way. It is a general term for all shipboard devices and networks such as ship energy generation, transmission, distribution and consumption. A typical ship electric propulsion system is shown in Fig. 1.

In an electric propulsion ship power grid, there are three sources of harmonics. The first source is the harmonics generated by power generation. The second is the harmonics

generated by the transmission and distribution systems. The third is the harmonics generated by electrical equipment. The harmonics mentioned above, which are generated by the supply and transmission of power and distribution systems, are designed with harmonic suppression in mind. In addition, the provided power supply can meet the power quality requirements of the electrical equipment. Therefore, this paper takes the harmonics generated by electrical equipment as its research object. The propulsion inverter is the main piece of electrical equipment and also the main harmonic source for a ship electric propulsion system.

The frequency of the harmonic current generated by the propulsion inverter with the n-pulse rectifier circuit is:

$$f = f_1(nk \pm 1),\ k=1, 2, \ldots \quad (1)$$

where f_1 is the fundamental frequency of 50Hz. For a propulsion inverter load with a 6-pulse rectifier circuit, the harmonic currents are of the 5th, 7th, 11th and 13th order. Therefore, four PDTFs (5th, 7th, 11th and 13th), which are connected in parallel with two harmonic sources, effectively eliminate the current harmonics of the ship electric propulsion system.

III. Method for Fully Tuning of a PDTF

Aiming at problems such as variations of the resonant frequency and filter characteristics, resonance point migration, and unstable filtering performances in conventional passive filters, a method for fully tuning of a PDTF is proposed. A method for the dynamic tuning of a PDTF is a key technology for the harmonic suppression of ship electric propulsion systems. The main research contents include: the topological structure, the control principle of a PDTFs, and a full tuning method based on the fundamental equivalent impedance and harmonic impedance.

A. Topological Structure of a PDTF

The core component of the PDTF is an ECRITHS. The primary reactance winding of the ECRITHS is connected in series with a filter capacitor group (FCG), the secondary control winding is connected a PEIC, and the secondary filter winding is connected with an IF designed to suppress the harmonics generated by the PEIC. Taking a single PDTF as an example, a block diagram is shown in Fig. 2.

In Fig. 2, Q_{01} is a circuit breaker, $FS_{1\sim n}$ is a fuse, $KM_{1\sim n}$ is a capacitor contactor, C_s is the equivalent capacitance of the FCG, L_s is the equivalent inductance of the primary reactance winding of the ECRITHS, and L_s and C_s constitute the resonant branch of the PDTF. In addition, NL is the harmonic source. The mechanism and control structure of the PDTF have been shown in [25]-[29].

The systematic control structure consists of a main circuit and a control system. The main circuit is mainly composed of

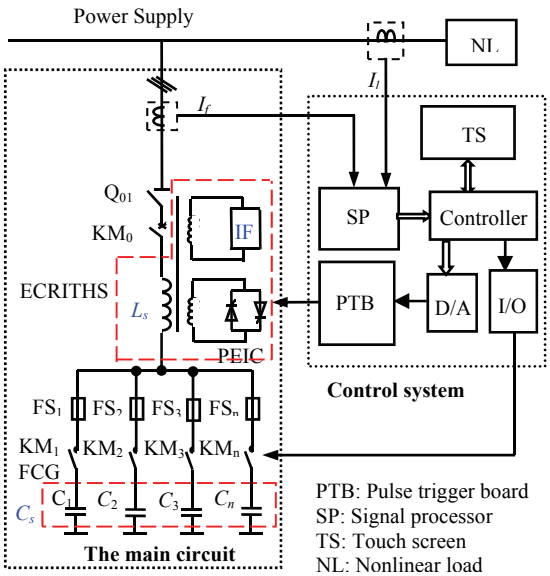

Fig. 2. Block diagram of a PDTF.

Q_{01}, ECRITHS, FCG, KM_0, $KM_{1\sim n}$ and $FS_{1\sim n}$. Among these, the ECRITHS is made up of a PEIC and an IF. The PEIC is a three-phase high impedance inverter that is constituted by six thyristors V_1~V_6 (V_1, V_3 and V_5 are connected at the cathode, while V_4, V_6 and V_2 are connected at the anode) and the reactance control winding of the PEIC. The thyristors are driven through phase control. According to the control principle of power electronic conversion technology, A-B, A-C, B-C, B-A, C-A and C-B correspond to thyristors V_1, V_3, V_5, V_4, V_6 and V_2, respectively. A pair of thyristors is triggered every 60 degrees to realize the impedance transformation of the three-phase high impedance inverter.

The control system consists of a harmonic sensor (SP), a controller, a thyristor pulse trigger board (PTB), a touch screen (TS), a D/A converter (D/A), a digital input and output (I/O), etc.

The control system collects information of the harmonics via the SP and makes control decisions such as data processing and filtering algorithm optimization via the controller. The results are output in two ways. One output is D/A, which controls the PEIC through the PTB, which realizes the transformation and continuous control of the electromagnetic parameters of the ECRITHS. The other output is I/O, which controls the dynamic switching of the FCG of the main circuit. The controller controls the signals output via these two ways to realize the tuning and filtering of harmonics.

B. Control Principle of the PDTF

According to the direction of the harmonic current in a power system, the detuning degree can be expressed by the harmonic current offset. In a power system, part of the harmonic current generated by a nonlinear load enters the filter branch, and part of it enters the grid side. When a PDTF works normally, it resonates at the harmonic frequency, which forms a low impedance bypass to the sub-harmonic current,

at which most of the harmonic current is absorbed by the PDTF. When the PDTF mistunes, the resonant frequency of its L_sC_s series circuit deviates from the harmonic frequency, and the PDTF electrically operates on the sub-harmonic current. When the tuning impedance of the current increases, the harmonic current generated by the load side flows into the power grid in large quantities. This reduces the harmonic current in the filter branch.

Set the h^{th} harmonic current offset ΔI_h:

$$\Delta I_h = I_{hl} - I_{hf} \tag{2}$$

where I_{nf} is the effective value of the h^{th} harmonic current of the PDTF branch, I_{nl} is the effective value of the h^{th} harmonic current of the NL. The detuning degree of the PDTF is described by the offset ΔI_h. When the filter is in resonance, the value of ΔI_h is close to 0. However, when the filter is detuning, the harmonic current offset ΔI_h increases, and the detuning degree also increases.

By synchronous sampling of the PDTF branch current I_f and load current I_l, the h^{th} harmonic current I_{hf} of the PDTF branch and the h^{th} harmonic current I_{hl} of the load are obtained. With the ΔI_h minimum as the control target, the controller controls the firing angle α of the thyristors in the PEIC.

At the fundamental frequency, the PDTF is mainly used to compensate the reactive power of the system. The capacitor can be input and removed dynamically and timely. Therefore, the overall capacitance reactance can be adjusted. In this way, the capacitor can be put into the system according to the actual needs, and the inductance of the ECRITHS can be adjusted. The PDTF can compensate the reactive power of the system without overcompensation.

At harmonic frequencies, the PDTF is mainly used to absorb harmonics. When the PDTF is in resonance, the controller keeps the firing angle α of the thyristors in the PEIC. When the capacity of the capacitor bank changes, for example, when the temperature changes and time passes, the capacity of the capacitor bank becomes smaller. If the inductance L_s remains unchanged, the actual resonance frequency f_h (such as f_5 = 250Hz, that is, the 5th harmonic resonance frequency) increases, and the filtering effect is greatly affected. However, the PDTF improves this situation. When the capacitor bank capacity changes, the controller adjusts the firing angle α of the thyristors in the PEIC, and the inductance L_s produced by the primary reactance winding changes. Thus, the inductance L_s of the ECRITHS can be dynamically adjusted so the product of L_sC_s remains unchanged and the filtering frequency f_h remains unchanged. As a result, the filtering accuracy and filtering effect are unaffected.

C. Full Tuning Method based on Fundamental Impedance and Harmonic Impedance

A schematic diagram of the connection between the PDTF and the NL is shown in Fig. 3.

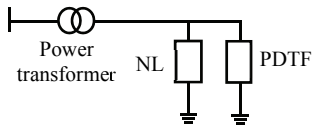

Fig. 3. Schematic diagram of the PDTF and NL connection.

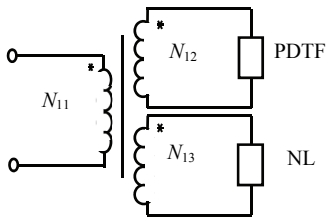

Fig. 4. Equivalent diagram of a PDTF connected to an NL.

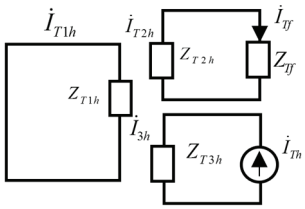

Fig. 5. Equivalent harmonic model of a power transformer and the PDTF connection.

As shown in Fig. 3, both the NL and the PDTF are connected to the secondary side of the power transformer. Therefore, an equivalent diagram of a PDTF connected to a nonlinear load can be obtained. According to the superposition principle, an equivalent diagram of a PDTF connected to a NL is shown in Fig. 4.

In Fig. 4, the power transformer is composed of a core, a primary winding, and a secondary winding. Among them, the power supply voltage is connected to the power supply winding N_{11}; and the winding connections of the PDTF and NL are called the filter winding N_{12}, and the non-linear load winding N_{13}, respectively. N_{13} winding turns are equal to N_{12} winding turns. N_{11} can be regarded as the primary winding, and N_{12} and N_{13} can be regarded as the secondary windings.

The harmonic source in the winding N_{13} is replaced by the current source $\dot{I}_{Th}$. Meanwhile the harmonic currents in the N_{11}, N_{12} and N_{13} windings are $\dot{I}_{T1h}$, $\dot{I}_{T2h}$ and $\dot{I}_{T3h}$, respectively. In addition, the harmonic current in the branch of the PDTF is $\dot{I}_{Tf}$. Assuming that the equivalent harmonic impedance of the windings N_{11}, N_{12} and N_{13} of the power transformer are Z_{T1h}, ZT2h and Z_{T3h}, the harmonic impedance of the PDTF is Z_{Tf}. An equivalent circuit can be obtained from Fig. 4, as shown in Fig. 5.

The relationship between the equivalent harmonic current of winding N_{11} and winding N_{13} is:

$$\dot{I}_{T1h} = \frac{N_{13}N_{11}(Z_{T2h}+Z_{Tf})}{N_{11}^{\ 2}(Z_{T2h}+Z_{Tf})+N_{12}^{\ 2}Z_{T1h}}\dot{I}_{Th} \tag{3}$$

It can be seen from Equ. (3) that for the h^{th} harmonic, as

long as the harmonic current in winding N_{11} of the transformer is equal to zero, it is necessary for:

$$Z_{T2h} + Z_{Tf} = 0 \tag{4}$$

The structure and parameters of the PDTF can be designed to satisfy Equ. (4). In this case, the harmonic current $\dot{I}_{T1h}$ can be zero in the ideal state. Therefore, the PDTF can completely suppress the harmonics generated by the NL.

The PDTF is designed according to the dynamic L-C parameters. This is the full-tuning method based on the fundamental equivalent impedance and the harmonic impedance.

IV. Harmonic Suppression Principle of the PDTF

The harmonics in a current waveform can be regarded as integer multiples at a certain fundamental frequency, e.g., $f_0 = 50$ Hz. Thus, $f_h = h \times f_0$, where h is the harmonic order.

Taking the harmonic current as an example, its expression is:

$$\begin{cases} \dot{I}_1 = \dot{I}_{m1} \sin(\omega_1 \times t) \\ \dot{I}_h = \dot{I}_{mh} \sin(h\omega_1 - \varphi_h) \end{cases} \tag{5}$$

where $\dot{I}_{m1}$ denotes the peak value of the fundamental current and $\dot{I}_{mh}$ is the peak value of the h^{th} harmonic current.

As can be known from Section II, for a propulsion inverter load with a 6-pulse rectifier circuit, the harmonic currents are of the 5th, 7th, 11th and 13th order. In other words, the values of h are 5, 7, 11 and 13. This shows that for the harmonics generated by a 6-pulse frequency converter, the 5th harmonic should be filtered first, followed by the 7th, 11th and 13th harmonics successively.

When the ECRITHS and the FCG are in series resonance in the PDTF, it is possible to obtain:

$$\frac{1}{h\omega_1 C_s} = h\omega_1 L_s \tag{6}$$

where ω_1 represents the fundamental angular frequency of the power grid. When the capacitance of the filter capacitor C_s decreases due to dielectric aging or other reasons, the resonant point of the PDTF can be returned to the harmonic frequency by adjusting the equivalent inductance L_s.

Under normal conditions, the resonant frequency is f_h (h=5, 7, 11 and 13), and the impedance of the filter branch is very small. When the capacitance of the filter capacitor C_s decreases, the resonant frequency f_h of the PDTF increases to f. Meanwhile, the resonant point gradually shifts to a higher frequency when the service time of the capacitor increases.

The total impedance Z_{hf} of the branch where the PDTF is located is:

$$Z_{hf} = R_{hf} + j\left(h\omega_1 L_s - \frac{1}{h\omega_1 C_s}\right) \tag{7}$$

When the reactor L_s and the capacitor C_s are in series resonance, the imaginary part in Equ. (7) is 0. Therefore:

$$h = \frac{1}{\omega_1 \sqrt{L_s C_s}} = \sqrt{\frac{X_{C1}}{X_{L1}}} \tag{8}$$

where X_{L1} and X_{C1} denote the inductive reactance value and the capacitive reactance value of the ECRITHS at the fundamental angular frequency ω_1 of the power grid.

The capacitance of the filter capacitor Q_C, the capacitance value C_s, the capacitance value X_C and the resonance frequency f_h are formulated as follows:

$$\begin{cases} X_{C1} = \dfrac{U^2}{Q_C} \\ C_s = \dfrac{1}{2\pi f_1 X_{C1}} \end{cases} \tag{9}$$

$$f_h = \frac{1}{2\pi\sqrt{L_s C_s}} = f_1 \sqrt{\frac{X_{Ch}}{X_{Lh}}} \tag{10}$$

where X_{Lh} and X_{Ch} represent the inductive reactance value and the capacitive reactance value of the ECRITHS at the resonant frequency f_h, respectively. If the capacity Q_C of the filter capacitor decreases, the capacitance reactance X_{C1} of the filter capacitor increases. However, C_s decreases, and the resonance frequency f_h increases. Thus, the PDTF deviates from the original resonance point and the accuracy of the filter declines. At this point, if L_s is properly increased, the PDTF can return to the previous resonance point.

The PDTF can dynamically filter the harmonic current of the corresponding order at the resonant frequency. It can also overcome the detuning caused by the change of the capacitance parameter or other reasons.

Reactive power compensation of the PDTF under the fundamental wave is another key issue. According to the reactive power of the system, the capacity of the input capacitor can be flexibly changed to prevent the system from reactive power under-compensation and over-compensation.

The impedance Z_{f1} of the PDTF under the fundamental wave is:

$$Z_{f1} = \frac{1}{\omega_1 C_s} - \omega_1 L_s = \frac{1}{\omega_1 C_s} \cdot \frac{h^2 - 1}{h^2} = X_{Cs1} \cdot \frac{h^2 - 1}{h^2} \tag{11}$$

where X_{Cs1} is the capacitance reactance value of the PDTF at the fundamental angular frequency.

According to Eqns. (9) and (10), the capacitive reactive power Q_P provided by the PDTF at the fundamental frequency is:

$$Q_P = \frac{U_1^2}{Z_{f1}} = \frac{Q_{CN} U_1^2}{U_{CN}^2} \frac{h^2}{h^2 - 1} \approx Q_{CN} \cdot \frac{h^2}{h^2 - 1} \tag{12}$$

where U_1 denotes the fundamental voltages at both ends of the filter capacitor, and U_{CN} and Q_{CN} are the rated voltage and capacity of the capacitor, respectively.

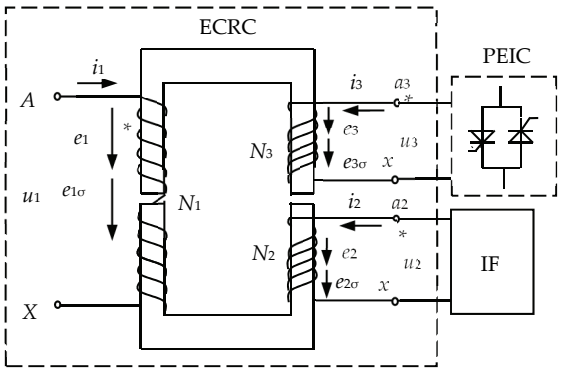

Fig. 6. Structure of the ECRITHS.

V. Characteristics of the ECRITHS

The PEIC is regulated by the thyristor three-phase full-control mode. In the process of impedance transformation, a certain amount of $6k\pm1$ (k=1, 2…) order harmonics is generated. For this reason, this paper invents an ECRITHS. The IF is designed to suppress the harmonics generated by the PEIC. Based on the structure of the ECRITHS, the mathematical equation of the harmonic influence coefficient is constructed. Using the MATLAB 2016b simulation tool, the harmonic suppression and the impedance transformation impedance transformation characteristics of the ECRITHS are simulated.

A. Structure of the ECRITHS

The ECRITHS is based on the electromagnetic coupling reactor (ECR) structure [10], with the secondary filtering winding N_2 added, as shown in Fig. 6.

In Fig. 6, a single winding iron core reactor is designed as an electromagnetic coupling reactance converter (ECRC) with the primary reactance winding N_1, the secondary filter winding N_2 and the secondary control winding N_3. N_3 is connected to the PEIC, and N_2 is connected to the IF, which forms a harmonic-free electromagnetic coupling reactor. The impedance transformation of the ECRITHS is realized by the PEIC, and the harmonic suppression of the ECRITHS is realized by the IF. A detailed graphic symbol description of the ECRITHS is given in Table II.

B. Mathematical Equation of the Harmonic Influence Coefficient

In order to facilitate the mathematical model analysis of the ECRITHS, a simplified equivalent circuit of the ECRITHS can be obtained by simplifying the structure of Fig. 6, as shown in Fig. 7.

In Fig. 7, assuming that there is no harmonic component in the primary reactance winding of the ECRC, the harmonic generated by the PEIC is replaced by the current source $\dot{I}_h$. In addition, the harmonic currents in the primary reactance winding N_1 , the secondary filter winding N_2 and the secondary control winding N_3 are $\dot{I}_{1h}$, $\dot{I}_{2h}$ and $\dot{I}_{3h}$. The harmonic currents

TABLE II
Detailed Graphic Symbol Description of the ECRITHS

Graphic symbol	Description
N_1(A, X)	Primary reactance winding of ECRC
N_2(a_2, x)	Secondary filter winding of ECRC
N_3(a_3, x)	Secondary control winding of ECRC
u_1, u_2, u_3	Voltage of N_1, N_2, N_3, respectively
i_1, i_2, i_3	Current of N_1, N_2, N_3, respectively
e_1, e_2, e_3	Inductive potential of N_1, N_2, N_3, respectively
$e_{1\sigma}$, $e_{2\sigma}$, $e_{3\sigma}$	Leakage potential of N_1, N_2, N_3, respectively

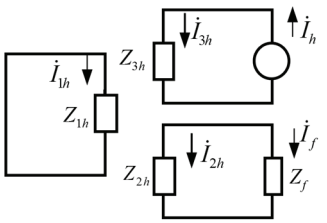

Fig. 7. Simplified equivalent circuit of the ECRITHS.

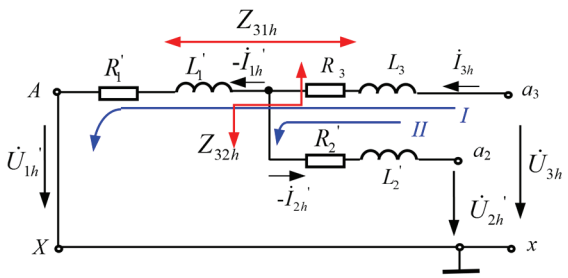

Fig. 8. Equivalent harmonic circuit of the ECRITHS.

absorbed by the IF is $\dot{I}_f$. The equivalent harmonic impedance of N_1, N_2, N_3 and IF are Z_{1h}, Z_{2h}, Z_{3h} and Z_f, respectively.

As shown in Fig. 7, the relationship between the h^{th} subharmonic current and the voltage is:

$$\begin{cases} \dot{I}_{3h} = \dot{I}_h \\ \dot{I}_{2h} = -\dot{I}_f \end{cases} \tag{13}$$

$$\begin{cases} \dot{U}_{1h} = 0 \\ \dot{U}_{2h} = \dot{U}_f = Z_f \dot{I}_f \end{cases} \tag{14}$$

The harmonic current and voltage of N_1 and N_2 are converted as follows:

$$\begin{cases} \dot{I}_{1h}' = \dfrac{N_1}{N_3}\dot{I}_{1h} \\ \dot{U}_{1h}' = \dfrac{N_3}{N_1}\dot{U}_{1h} \\ \dot{I}_{2h}' = \dfrac{N_2}{N_3}\dot{I}_{2h} = -\dfrac{N_2}{N_3}\dot{I}_f \\ \dot{U}_{2h}' = \dfrac{N_3}{N_2}\dot{U}_{2h} = \dfrac{N_3}{N_2}\dot{U}_f \end{cases} \tag{15}$$

Without taking the excitation current into consideration, the equivalent harmonic circuit corresponding to Fig. 7 is obtained, as shown in Fig. 8.

TABLE III
HARMONIC EQUIVALENT IMPEDANCE RELATIONSHIP OF THE ECRITHS

Serial Number	Position	Harmonic equivalent impedance	Turn ratio relationship
1	N_1 and N_2	$Z_{12h}=Z_{21h}=Z_{12h}'$	Reciprocal
2	N_1 and N_3	$Z_{13h}=Z_{31h}$	Reciprocal
3	N_2 and N_3	$Z_{23h}=Z_{32h}=Z_{23h}'$	Reciprocal

From Fig. 8, the equivalent harmonic impedance relation of the ECRITHS can be obtained as follows:

$$\begin{cases} Z_{1h}' = \frac{1}{2}(Z_{12h}+Z_{13h}-Z_{23h}') \\ Z_{2h}' = \frac{1}{2}(Z_{21h}+Z_{23h}-Z_{13h}') \\ Z_{3h} = \frac{1}{2}(Z_{31h}+Z_{32h}-Z_{12h}') \end{cases} \tag{16}$$

where the harmonic equivalent impedance relationships of the ECRITHS are shown in Table III.

According to the KCL equation of the node, the equation of the zine potential of the h^{th} harmonic current can be obtained as:

$$\dot{I}_{3h}-\dot{I}_{1h}'-\dot{I}_{2h}'=0 \tag{17}$$

Using the superposition principle, the following voltage equation is obtained from Fig. 8:

$$\begin{cases} \dot{U}_{3h}-\dot{U}_{1h}' = -\dot{I}_{1h}'Z_{31h}-\dot{I}_{2h}'Z_{3h} \\ \dot{U}_{3h}-\dot{U}_{2h}' = -\dot{I}_{2h}'Z_{32h}-\dot{I}_{1h}'Z_{3h} \end{cases} \tag{18}$$

Substituting Eqns. (13)-(15) into Equ. (18) yields:

$$\begin{cases} \dot{U}_{3h} = -\frac{N_1}{N_3}\dot{I}_{1h}Z_{31h}-\frac{N_2}{N_3}\dot{I}_{2h}Z_{3h} \\ \dot{U}_{3h} = +\frac{N_3}{N_2}Z_f\dot{I}_{2h}-\frac{N_2}{N_3}\dot{I}_{2h}Z_{32h}-\frac{N_1}{N_3}\dot{I}_{1h}Z_{3h} \end{cases} \tag{19}$$

Simplifying Equ. (19) yields:

$$\frac{N_3}{N_2}Z_f\dot{I}_{2h}-(-Z_{32h}+Z_{3h})\frac{N_2}{N_3}\dot{I}_{2h}=(-Z_{3h}+Z_{31h})\frac{N_1}{N_3}\dot{I}_{1h} \tag{20}$$

From Equ. (20):

$$\dot{I}_{2h}=\frac{\frac{N_1}{N_3}(Z_{3h}-Z_{31h})}{\frac{N_2}{N_3}(Z_{3h}-Z_{32h})-\frac{N_3}{N_2}Z_f}\dot{I}_{1h} \tag{21}$$

Substituting Equ. (16) into Equ. (21) yields:

$$\dot{I}_{2h}=\frac{\frac{N_1}{N_3}\frac{1}{2}(Z_{31h}-Z_{32h}+Z_{12h}')}{\frac{N_2}{N_3}\frac{1}{2}(-Z_{31h}+Z_{32h}+Z_{12h}')+\frac{N_3}{N_2}Z_f}\dot{I}_{1h} \tag{22}$$

The harmonic equivalent impedance relationship of the electromagnetically coupling reactor shown in Table III is substituted into Equ. (22) and simplified:

$$\dot{I}_{2h}=\frac{N_2}{N_1}\frac{Z_{1h}}{Z_{2h}+Z_f}\dot{I}_{1h} \tag{23}$$

Substituting Eqns. (15) and (23) into Equ. (21), and simplifying them yields the harmonic influence coefficient K_h:

$$K_h=\frac{\dot{I}_{1h}}{\dot{I}_h}=\frac{N_3N_1(Z_{2h}+Z_f)}{N_1^2(Z_{2h}+Z_f)+N_2^2Z_{1h}} \tag{24}$$

Equ. (24) reveals the relationship between the equivalent harmonic currents of N_1 and N_3. The harmonic influence of the harmonic source generated by the PEIC on N_3 is related to K_h, as in the following.

(1) When K_h=0, $Z_{2h}+Z_f$=0 and I_{1h}=0, it is indicated that the IF has the best harmonic suppression effect.

(2) When 0<K_h<1: the smaller the value of K_h, the smaller the influence. On the other hand, the larger the value of K_h, the greater the influence.

(3) When K_h=1 and $I_{1h}=I_h$, the influence is the greatest.

Therefore, it can be concluded that as long as the sum of the harmonic impedance Z_{2h} of N_2 and the impedance Z_f of the IF is zero, the IF can completely suppress the harmonic current generated by the PEIC.

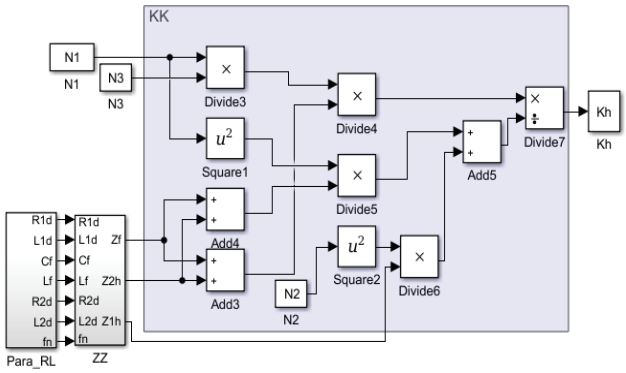

Fig. 9. Simulation model of the harmonic suppression characteristics of the ECRITHS.

C. Simulation of the Harmonic Suppression Characteristics of the ECRITHS

A simulation model of the harmonic suppression characteristics of the ECRITHS is constructed according to Eq. (24), as shown in Fig. 9.

Taking the filtering of the 5th harmonic current as the research object, an L_fC_f passive filter is used in the IF, where the capacitor selected is 10 kVar, and the capacitor voltage is 525V. The harmonic suppression characteristics of the ECRITHS are simulated and analyzed, including a relationship curve between the harmonic influence coefficient K_h and the IF impedance Z_f, as shown in Fig.10.

From Fig. 10, the validity of formula (24) is verified. The influence of the harmonic source produced by N_3 on the

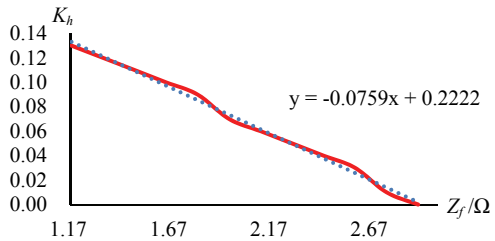

Fig. 10. Relation curve between the harmonic influence coefficient K_h and the IF impedance Z_f.

TABLE IV
DESIGN PARAMETERS OF THE ECRITHS

Basic parameters	Number of turns	1: 5
	capacity /kVA	5
Primary reactance winding N_1	N_1	40
	Current I_1/A	75
	Voltage U_1/V	38
	Inductance L_1' /mH	1.62
	Resistance R_1' /Ω	0.0324
Secondary harmonic winding N_2	N_2	200
	Current I_2/A	15
	Voltage U_2/V	190
	Inductance L_2' /mH	1.852
	Resistance R_2' /Ω	0.0369
Secondary control winding N_3	N_3	200
	Current I_3/A	15
	Voltage U_3/V	190
	Inductance L_3/mH	1.852
	Resistance R_3/Ω	0.0369

harmonic of N_1 is related to K_h. The harmonic influence coefficient K_h decreases linearly with the increase of Z_f, with its slope determined by the parameters of the ECRITHS. Therefore, it can be concluded that the harmonic current generated by N_3 can be completely absorbed by the IF, if Z_f can be adjusted to make K_h close to 0.

D. Simulation of the Impedance Transformation Characteristics of the ECRITHS at the Fundamental Frequency

Firstly, an impedance transformation simulation model of the ECRITHS is constructed according to the impedance transformation mathematical model of the ECRITHS. Then an impedance transformation characteristic curve of the ECRITHS is obtained by simulation.

When the PEIC operates between the "open state and the short circuit state" with the excitation current (Z_m=∞) being ignored, the impedance transformation mathematical model of the ECRITHS [10] is as follows:

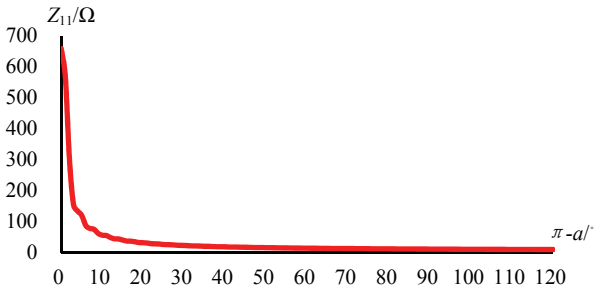

Fig. 11. Impedance transformation characteristic curve of the ECRITHS.

TABLE V
IMPEDANCE CONVERSION CHARACTERISTICS OF THE ECRITHS

π -α/°	Z_{11}/Ω	Characteristics description
0	Maximum	N_3 of ECRC is short-circuited
0～10	Rapid decrease	
10～30	Change significantly	$Z_{11min} \le Z_{11} \le Z_{11max}$
30～120	Change slowly	
120	Minimum	N_3 of ECRC is open-circuited

$$\begin{cases} Z_{11} = Z_1' + Z_3 + Z_\alpha \\ Z_a = \dfrac{U_3}{I_3} = \dfrac{\pi Z_3}{\sqrt{\sin^2 a + (\pi - a)\sin 2a + (\pi - a)^2}} \end{cases} \tag{25}$$

An impedance transformation simulation model of the ECRITHS is constructed according to Equ. (25). According to the simulation of design parameters of the ECRITHS in Table IV, an impedance transformation characteristic curve of the ECRITHS at the fundamental frequency is obtained, as shown in Fig. 11.

The following conclusions can be verified from Fig. 11. The ECRITHS is equivalent to a reactor with a variable inductance. The impedance conversion characteristics of the ECRITHS are shown in Table V.

VI. SIMULATION AND EXPERIMENTAL EVALUATION OF THE PDTF

A. Simulation evaluation of the PDTF

Numerical simulations have been conducted to validate the PDTF used for the harmonic suppression of a ship electric propulsion system. A simulation model for the harmonic suppression of a ship electric propulsion system is constructed according to the above research results, as shown in Fig. 12.

In Fig. 12, the implement three-phase source is selected as the Power Supply (PS), with speed and load torque set by the SV module. Signals are saved and scoped by the SS module. The harmonics are produced by two FOCIMDs, which are used to drive propellers 1 and 2 (see in Fig. 2). The three-phase inverter in Fig. 12(b) is the propulsion inverter with a 6-pulse rectifier circuit. Therefore, the PDTF consisting of

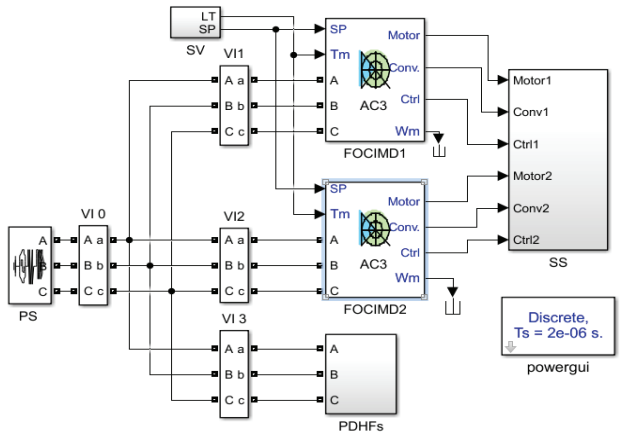

(a)

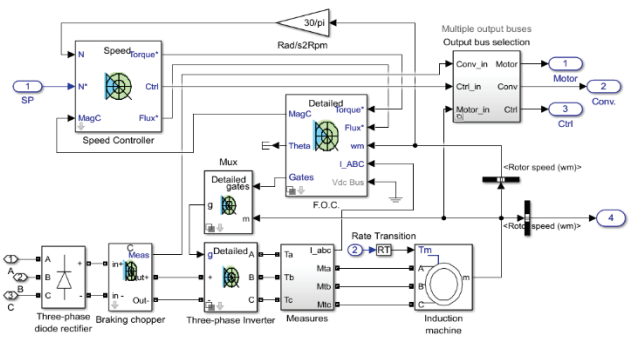

(b)

Fig. 12. Simulation model for the harmonic suppression of a ship electric propulsion system. (a) Simulation model. (b) Simulink schematic of a field-oriented control induction motor drive (FOCIMD).

TABLE VI
SIMULATION PARAMETERS OF THE INDUCTION MOTOR

Electrical Parameters	Power/kVA	149.2
	Voltage/V	460
	Frequency/Hz	50
Equivalent circuit values	Resistance/Ω(Stator)	14.85×10-3
	Leakage inductance/mH (Stator)	0.3027
	Resistance/Ω(Rotor)	9.295×10-3
	Leakage inductance/mH (Roator)	0.3027
	Mutual inductance/mH	10.46
Mechanical Parameters	Inertia/kg*m^2	3.1
	Friction	0.08
	Pole Pairs	2

four PDTFs (5th, 7th, 11th and 13th) are connected in parallel with the two harmonic sources (FOCIMD 1 and 2). Four PDTFs have been applied to eliminating the harmonics of a ship power system with the proposed method for dynamic tuning of the PDTF in the above simulation system.

According to the simulation parameters of the induction motor in Table VI, the speed reference is set to 1000rpn, and load torque is set to 792NM. Using a Powergui FFT Analysis Tool, simulated results of the 5th, 7th, 11th and 13th harmonic currents and the THD in the source current (VI$_0$) with and without the PDTF are shown in Table VII. In addition, current curves in the VI$_0$ with and without the PDTF are shown in Fig. 13.

TABLE VII
SIMULATED RESULTS OF HARMONIC SUPPRESSION

Harmonic order	Cs/uF	Ls/mH	Harmonic Current /A		
			without PDTF	With PDTF	Absorption
5th	1501.5	0.270	138.11	19.31	118.8
7th	693	0.298	75.98	17.46	58.52
11th	288.75	0.290	14.46	9.43	5.03
13th	115.5	0.519	15.60	8.79	6.81
THD /%	-		67.34	4.64	-

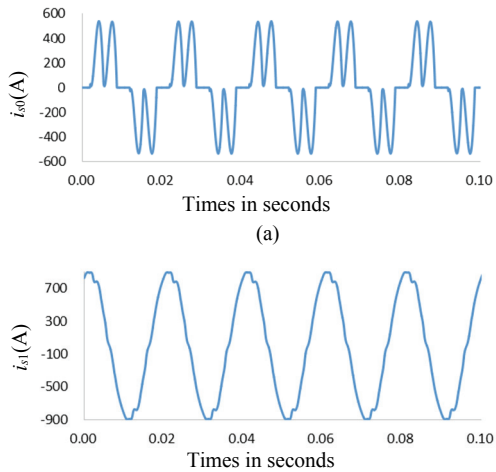

Fig. 13. Current curve in the VI$_0$. (a) Without the PDTF. (b) With the PDTF.

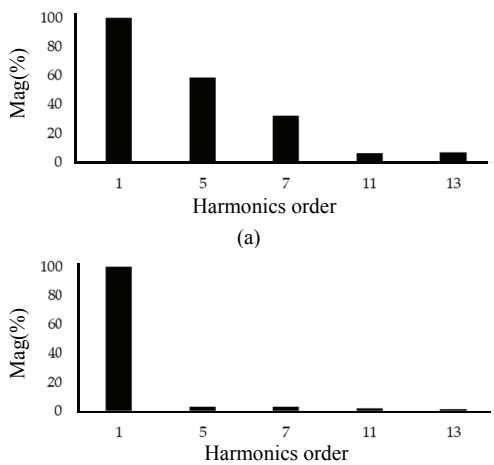

Fig. 14. Magnitudes of the harmonic spectrum in the VI$_0$. (a) Without the PDTF. (b) With the PDTF.

As can be seen, the current i_{s0} (Fig. 13(a)) in the VI$_0$ without the PDTF contains a significant number of harmonics, and the current i_{s1} (Fig. 13(b)) in the source current with the PDTF contains a lot fewer harmonics than i_{s0}. The magnitudes of the harmonic spectrum are shown in Fig. 14.

Fig. 15. Pictures of the PDTF.

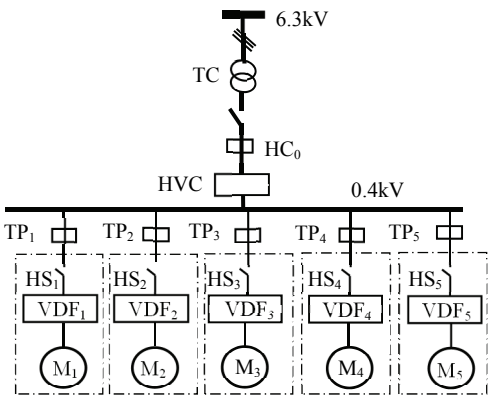

Fig. 16. Schematic diagram of the main electrical configuration in a distribution system.

The following conclusions can be verified from Table VII, Fig. 13 and Fig. 14. The THD of the source current is 67.34%, which is reduced to about 4.64% by the multi-order simultaneous dynamic filtering. At the same time, the harmonic current can be absorbed by the PDTF, with the absorption efficiency rate of the 5th harmonic current being above 80%. It has been found that multiple PDTFs can be configured to realize multi-order simultaneous dynamic filtering, and can reduce the THD of source currents well below the 5% limit of the IEEE-519 standard [11].

B. Experimental Evaluation of the PDTF

Pictures of the PDTF are shown in Fig. 15, and it has been applied to eliminate the harmonics of a low voltage distribution system, with a transformer capacity of 1250kVA and a ratio of 6.3kV/0.4kV. There are five harmonic sources (HS_1- HS_5) in different geographic places. The harmonics are produced by five variable-frequency drives (VFD_1-VFD_5), which are used to drive the motors (M_1-M_5), respectively. A configuration diagram of the main electric cabinet is shown in Fig. 16.

The 5th harmonic current (I_5), THD, fundamental current (I_1) in the HC_0 and TP_1~ TP_5 are measured using a power quality analyzer (CA8335), where the measurement results of the distribution system are shown in Table VIII.

Five PDTFs are connected in parallel with five harmonic sources (HS_1- HS_5) (See Fig. 16 for details). Graphs of the 5th harmonic current (I_5) and its total harmonic distortion (THD) in the HC_0 are shown in Fig. 17.

TABLE VIII
MEASUREMENT RESULTS OF THE DISTRIBUTION SYSTEM WITHOUT THE PDTF

Test point	Rated Power/kW	I_1/A	I_5/A	THD/%
HC_0	-	1365	97	7.2
HC_1	75	93.2	29.6	31.7
HC_2	75	72.4	26.6	41.2
HC_3	75	96.6	30.4	32.8
HC_4	75	102.2	30.4	32
HC_5	50	86	25.4	29

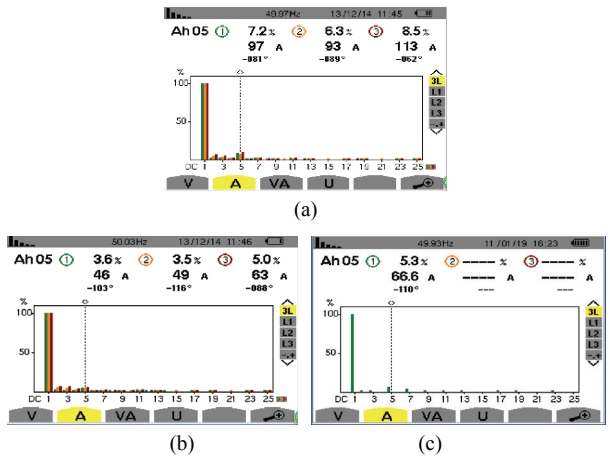

(a) (b) (c)

Fig. 17. Graphs of I_5 and THD in the HC_0. (a) I_5 and THD before filtering. (b) I_5 and THD with the PDTF. (c) I_5 and THD with a PPF.

Filtering performances of the PDTF and a PPF as shown in Fig.17 (taking phase A as an example) are as follows.

(1) Before filtering (Fig. 17(a)), the 5th harmonic current and the THD of the nonlinear load are 97A and 7.2%, respectively.

(2) With the dynamic filtering method (PDTF) proposed in this paper (Fig. 17(b)), the 5th harmonic current and the THD are reduced to 46A and 3.6%, respectively. The PDTF absorbed 51A of the 5th harmonic current. The absorption rate is 52.6%. The THD decreased by 50%.

(3) By the traditional passive filtering method (PPF), the 5th harmonic current and current distortion rate are 66.6A and 5.3%, respectively. The PPF absorbed 30.4A of the 5th harmonic current. The absorption rate is 33.4%. The THD decreased by 26.3%.

It can be seen from the above results that, under the same nonlinear load, the dynamic filtering method proposed in this paper is superior to the traditional passive filtering method and that its filtering performance is excellent.

The PDTF has been proposed to eliminate harmonic currents at different geographic places to comply with the IEEE-519 harmonic standard [11] by using a low voltage distribution

system. It has been found that the PDTF can effectively eliminate current harmonics in different geographic places. It has been shown that the PDTF is able to reduce the THD of supply currents to well below the 5% limit prescribed by the IEEE-519 standard.

VII. CONCLUSIONS

According to the harmonic characteristics of a ship electric propulsion system, their treatment methods and effective measurements have been studied to suppress and prevent the ship power system from affecting ship operation due to the serious damage caused by harmonics. By analyzing the PDTF, the control principle is discussed in detail. In addition, a method for fully tuning of the PDTF is proposed. Through the structure design of the ECRITHS and harmonic influence coefficient modeling, simulation evaluations are completed. The ECRITHS is equivalent to a reactor with a variable inductance. The designed IF can suppress the harmonics generated by the PEIC. It can be concluded that the harmonic current generated by the PEIC can be completely absorbed by the IF, if K_h can be adjusted close to 0. Experiments on the harmonic suppression of a ship electric power propulsion system have been completed. Multiple PDTFs can be configured to realize multi-order simultaneous dynamic filtering, and can effectively eliminate the current harmonics of the ship electric propulsion system to reduce the THD of the supply currents to well below the 5% limit prescribed by the IEEE-519 standard [11]. The PDTFs can also eliminate harmonic currents in different geographic places. It has been shown that the PDTF is able to reduce the THD of supply currents to well below the 5% limit specified by the IEEE-519 standard.

It is believed that this research is promising when a sufficiently developed technological basis is available. In order to further eliminate the detuning caused by filter capacitor capacity variation, an analysis and discussion should be made on the influence of the harmonic suppression of different filter capacitors on ship electric propulsion systems in future studies.

ACKNOWLEDGMENT

This work was supported by the National Support Program of China (#2015BAG20B05), the Zhejiang Province Natural Science Foundation of China (#LY14E070003), and the Independent Innovation Fund Project of Wuhan University of Technology (#2018-JL-004).

REFERENCES

[1] Y. Zhang, P. X. Yang, and L. Chen, "Harmonic characteristic research of the synchronous generator propulsion converter system in electric propulsion," *Ship Eng.*, Vol. 31, No. z1, pp. 98-101, Jul. 2009.

[2] D. R. Zhang, "Design and simulation of harmonic suppressor for multiphase rectifier in marine electric propulsion system," *Ship Sci. Technol*., Vol. 38, No. 12A, pp. 43-45, Dec. 2016.

[3] X. Xu and Q. Shi, "Power quality improvement method in marine electric propulsion system," *Electr. Eng*., No. 8, pp. 54-57, Aug. 2010.

[4] J. S. Kim and S. H. Kim, "Harmonic analysis of power conversion system for torque and speed changing of electric propulsion ship," *J. Korean Soc. Mar. Environ. Saf*., Vol. 17, No. 1, pp. 83-88, Mar. 2011.

[5] P. Xiao, G. K. Venayagamoorthy, and K. A. Corzine, "Seven-level shunt active power filter for high-power drive systems," *IEEE Trans. Power Electron*., Vol. 24, No. 1, pp. 6-13, Jan. 2009.

[6] D. Li, K. Yang, Z. Q. Zhu, and Y. Qin, "A novel series power quality controller with reduced passive power filter," *IEEE Trans. Ind. Electron*., Vol. 64, No. 1, pp. 773-784, Jan. 2017.

[7] R. N. Beres, X. Wang, M. Liserre, F. Blaabjerg, and C. L. Bak, "A review of passive power filters for three-phase grid-connected voltage-source converters," *IEEE J. Emerg. Sel. Topics Power Electron*., Vol. 4, No. 1, pp. 54-69, Mar. 2016.

[8] Y. Wang, Y. Yuan, J. Chen, and Q. Cheng, "A dynamic reactive power compensation method of super high-power and high-voltage motor," *Appl. Mech. Mater*., Vols. 602-605, pp. 2828-2831, Aug. 2014.

[9] E. Skjong, J. A. Suul, A. Rygg, T. A. Johansen, and M. Molinas, "System-wide harmonic mitigation in a diesel electric ship by model predictive control," *IEEE Trans. Ind. Electron*., Vol. 63, No. 7, pp. 4008-4019, Jul. 2016.

[10] Y. Wang, Y. Yuan, and J. Chen, "A novel electromagnetic coupling reactor based passive power filter with dynamic tunable function," *Energies*, Vol. 11, No. 7, pp. 1647-1665, Jun. 2018.

[11] P. E. C. Stone, J. Wang, R. Dougal, and Y. J. Shin, "Strategic harmonic filter placement in an electric ship integrated power system," *Nav. Eng. J*., Vol. 128, No. 1, pp. 35-46, Mar. 2016.

[12] O. F. Kececioglu, H. Acikgoz, and M. Sekkeli, "Advanced configuration of hybrid passive filter for reactive power and harmonic compensation," *Springer Plus*, Vol. 5, No. 1, pp. 1228-1247, Aug. 2016.

[13] S. H. E. A. Aleem, M. E. Balci, and S. Sakar, "Effective utilization of cables and transformers using passive filters for non-linear loads," *Int. J. Electr. Power Energy Syst*., Vol. 71, pp. 344-350, Oct. 2015.

[14] A. M. Othman and H. A. Gabbar, "Enhanced microgrid dynamic performance using a modulated power filter based on enhanced bacterial foraging optimization," *Energies*, Vol. 10, No. 6, pp. 776-788, Jun. 2017.

[15] M. Mohammadi, A. M. Rozbahani, and M. Montazeri, "Multi criteria simultaneous planning of passive filters and distributed generation simultaneously in distribution system considering nonlinear loads with adaptive bacterial foraging optimization approach," *Int. J. Electr. Power Energy Syst*., Vol. 79, pp. 253-262, Jul. 2016.

[16] S. P. Litran and P. Salmeron, "Analysis and design of different control strategies of hybrid active power filter based on the state model," *IET Power Electron*., Vol. 5, No.

8, pp. 1341-1350, Sep. 2012.
[17] M. Kale and E. Ozdemir, "An adaptive hysteresis band current controller for shunt active power filter," *Electr. Power Syst. Res*., Vol. 73, No. 2, pp. 113-119, Feb. 2005.
[18] J. Fang, H. Li, and Y. Tang, "A magnetic integrated LLCL filter for grid-connected voltage-source converters," *IEEE Trans. Power Electron.*, Vol. 32, No. 3, pp. 1725-1730, Mar. 2017.
[19] J. C. Leite, I. P. Abril, M. E. D. L. Tostes, and R. C. L. D. Oliveira, "Multi-objective optimization of passive filters in industrial power systems," *Electr. Eng*., Vol. 99, No. 1, pp. 387-395, Mar. 2017.
[20] V. S. R. V. Oruganti, A. S. Bubshait, V. S. S. S. S. Dhanikonda, and M. G. Simoes, "Real-time control of hybrid active power filter using conservative power theory in industrial power system," *IET Power Electron*., Vol. 10, No. 2, pp. 196-207, Feb. 2017.
[21] T. Ericsen, N. Hingorani, and Y. Khersonsky, "Power electronics and future marine electrical systems," *IEEE Trans. Ind. Appl*., Vol. 42, No. 1, pp. 155-163, Jan. 2006.
[22] N. He, D. Xu, and L. Huang, "The application of particle swarm optimization to passive and hybrid active power filter design," *IEEE Trans. Ind. Electron*., Vol. 56, No. 8, pp. 2841-2851, Aug. 2009.
[23] Y. Tang, P. C. Loh, P. Wang, F. H. Choo, F. Gao, and F. Blaabjerg, "Generalized design of high performance shunt active power filter with output LCL filter," *IEEE Trans. Ind. Electron*., Vol. 59, No. 3, pp. 1443-1452, Mar. 2012.
[24] H. H. Zeineldin and A. F. Zobaa, "Particle swarm optimization of passive filters for industrial plants in distribution networks," *Electr. Power Compon. Syst*., Vol. 39, No. 16, pp. 1795-1808, Oct. 2011.
[25] Y. Wang and Y. Yuan, "Development of a soft starter with current-limiting, reactive power compensation and harmonic filtering," *Appl. Mech. Mater*., Vols. 462-463, pp. 658-661, Nov. 2013.
[26] Y. Wang, Y. Yuan, Y. Chang, and Y. Xu, "A novel soft starting integration method with current-limiting, reactive power compensation for super high-power and high-voltage motor and harmonic filtering," *J. Wuhan. Univ. Technol*., Vol. 35, No. 7, pp. 140-143, Jul. 2013.
[27] Y. Wang and Y. Yuan, "A dynamic reactive power compensation method for high-power and high-voltage electronic motors based on self-adaptive fuzzy pid control," in *Proceedings of the 2016 IEEE Chinese Guidance, Navigation and Control Conference*, pp. 10-15, 2016.
[28] J. Chen, L. Xiao, Y. Yuan, K. Yang, L. Lei, B. Mao, and Z. Chen, "Development of Passive dynamic power filter based on MCU," J. *Wuhan. Univ. Technol*., Vol. 35, No. 2, pp. 144-146, Feb. 2013.
[29] J. Li, J. Chen, Y. Deng, and J. Li, "Modeling and simulation of passive dynamic harmonic filter based on IGBT," *Appl. Mech. Mater.*, Vols. 475-476, pp. 1615-1618, Dec. 2013.

Yifei Wang was born in Chongqing, China, in 1990. He received his M.S. degree in Control Science and Engineering from the Wuhan University of Technology, Wuhan, China, in 2013, where he is presently working towards his Ph.D. degree. In 2017, he was invited to spend two years conducting joint training as a Visiting Ph.D. Student at the University of Wisconsin-Madison, Madison, WI, USA. His current research interests include power electronic, computer control and harmonic suppression.

Youxin Yuan was born in Hubei, China, in 1953. In 1977, he became an Assistant Teacher in the Department of Automation, Wuhan University of Technology, Wuhan, China, where he became an Associate Professor in 1991, and where he has been a Professor and Doctoral Supervisor since 2001 and 2006, respectively. His current research interests include power electronics, reactive power compensation and harmonic suppression.

Jing Chen was born in Chongqing, China, in 1965. She received her M.S. and Ph.D. degrees from the Wuhan University of Technology, Wuhan, China, in 1997 and 2003, respectively. She is presently working as a Full Professor in the School of Automation, Wuhan University of Technology, Wuhan, China, where she has been a Professor and Doctoral Supervisor since 2004 and 2008, respectively. Her current research interests include control science and engineering, computer control, reactive power compensation and harmonic suppression.